Post-synthetic sulfonation of a diphenylanthracene based porous aromatic framework

ORIGINAL ARTICLE

A C G publications

Org. Commun. 15:4 (2022) 346-355

organic communications

Post-synthetic sulfonation of a diphenylanthracene based porous aromatic framework

Hakan Bildirir[*ψ]

Department of Chemistry and Chemical Engineering, Chalmers University of Technology, 412 96 Göteborg, Sweden

(Received October 14, 2022; Revised November 03, 2022; Accepted November 21, 2022)

Abstract: Post-synthetic modification is an alternative pathway to introduce functionalities into the backbone of porous materials. Sulfonation of porous organic polymers is one of the frequently applied post-functionalization since the sulfonate groups are interesting for various applications such as carbon dioxide storage, proton conduction, ion removal. Moreover, sulfonation drastically improve hydrophilicity of the hydrophobic materials, therefore, makes the final compounds more processable in aqueous media. In this article, a procedure for post-synthetic sulfonation of a diphenylanthracene (DPA) based porous aromatic framework (DPA-PAF) is presented. Oleum (fuming sulfuric acid) was used as the sulfonation agent in acetic acid+water media instead of the conventionally used chlorosulfonic acid in the chlorinated solvents. Aside from macroscopic (visual) observations such as improved dispersibility in water when compared to the parent compound, the introduction of sulfonate groups was confirmed by using infrared spectroscopy, elemental analysis, and gas sorption (surface area) measurements.

Keywords: Porous organic polymers; porous aromatic frameworks; PAF-1; post-synthetic modification; sulfonation; oleum.

1. Introduction

Porous materials provide high accessible surface areas, and categorized to three main categories depending on their building blocks; fully inorganic, organic-inorganic hybrid, fully organic porous materials.[1] Each sub-class of porous materials have their advantages and disadvantages, therefore, are utilized accordingly. For example, fully inorganic porous materials such as zeolites are very hydrothermally stable compounds, hence their success in high-temperature applications (e.g. cracking of hydrocarbons).[2] On the other hand, metal-organic frameworks (MOFs) are the flagship of hybrid porous materials, and perfect for the applications requiring very high surface area.[3,4] Finally, porous organic polymers are the main actors of solely organic porous materials, and are particularly interesting for electronic applications (e.g. sensing, heterogeneous photo(electro)catalysis, organic electronics).[5–7]

Porous organic polymers can be produced either in crystalline or amorphous forms depending on the reaction technique; solvothermal methods are employed to obtain the crystalline morphology (e.g. covalent organic frameworks (COFs)) whereas the standard put-and-stir techniques yield the amorphous porous organic polymers (e.g. conjugated microporous polymers CMPs), porous aromatic frameworks (PAFs)).[8] As a result of high amount of crosslinking via rigid and angled (co)monomers

[*] E-Mail: hakanbildirir@gmail.com

[ψ] Current address of the author: Photoactivated/Electrochemical Processes Units, IMDEA Energy, 28935, Mostoles/Spain

The article was published by ACG Publications
http://www.acgpubs.org/journal/organic-communications © October-December 2022 EISSN:1307-6175
DOI: http://doi.org/10.25135/acg.oc.138.2210.2605
Available online: December 01, 2022

(tectons) to create porosity along the skeleton, porous organic polymers are generally non-soluble.[9] Even though such behavior is defined as disadvantageous for many applications since it leads to poor mobility in the media and lack of solution-processability, their large accessible surface areas providing high number of contact points with the target compounds compensate these shortcomings.[10] For example, thioxanthone based porous organic polymers exhibited better catalytic properties despite the heterogeneity when compared to the molecular thioxanthone, which operates homogenously.[11] Furthermore, the insolubility can be turned to an advantage since it allows to isolate the non-soluble material by simple filtration or centrifugation.[11,12] However, a proper dispersion of the materials in the corresponding media is crucial for efficient performances, for which physical stimulus such as exfoliation, grinding or chemical modifications (e.g. introducing side groups) are commonly used.[13,14] Particularly for the applications in water, hydrophobicity of the organic backbone of the porous organic polymers is a drawback, therefore, increasing the hydrophilicity leads to a better processability.[15,16] For example, introduction of hydrophilic groups improved the efficiency of the materials for photocatalytic water splitting due to more interactions with the target compound thanks to the better dispersibility.[17]

Post-synthetic modification of porous organic polymers is a popular pathway to introduce further functionalities to the polymeric backbone.[18] Sulfonation as post-synthesis is one of the frequently applied post-synthetic reactions since sulfonate groups can improve the efficiency of the material for many applications (e.g. CO_2 sorption/storage, ammonia capture, ion exchange, proton conduction).[19–22] In addition to these, sulfonate groups improve the wettability of the hydrophobic backbone, therefore, sulfonated compounds are better processible in aqueous media when compared to their plain (hydrophobic) analogues.[22,23] The frequently followed pathway for post-synthetic sulfonation is through chlorosulfonic acid treatment in methylene chloride solution.[22–28] There are a few examples of sulfonation taking place in sulfuric acid and fuming sulfuric acid, which is considered as more environmentally friendly since the reactions do not require chlorinated solvents.[29–32] Moreover, in the literature, comparison of both pathways showed that oleum driven sulfonation was more efficient with respect to chlorosulfonic acid method.[32]

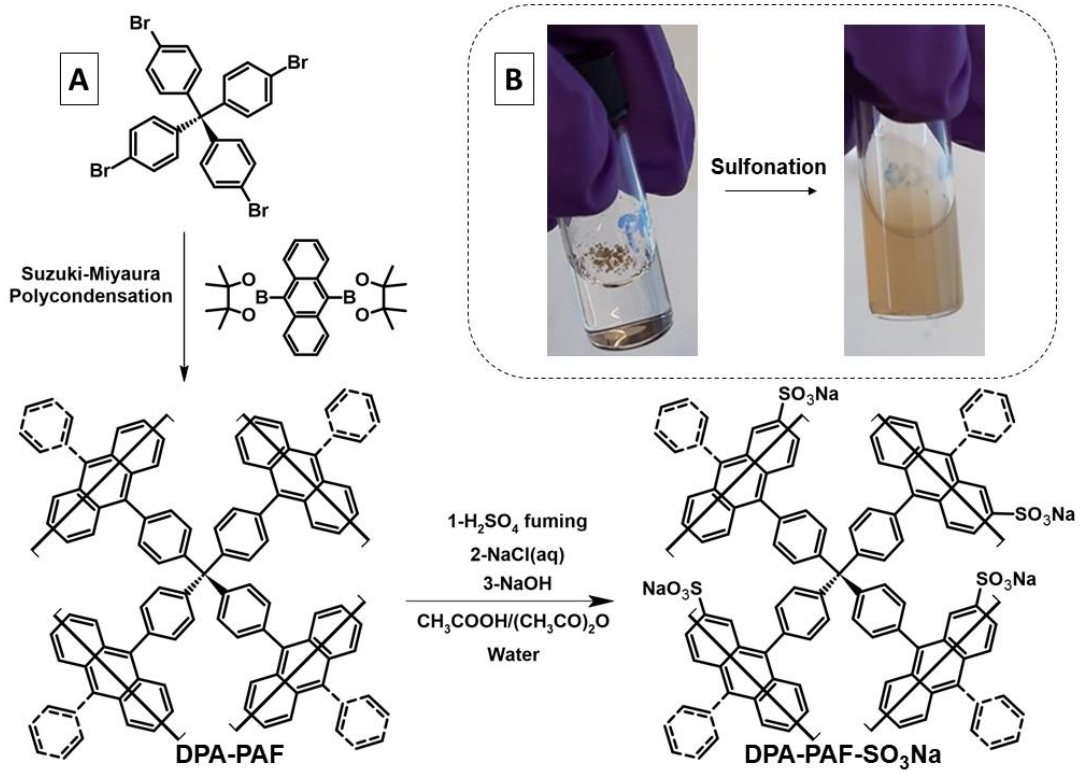

Figure 1. Synthesis of DPA-PAF and its post-synthetic sulfonation to form DPA-PAF-SO_3Na (**A**). The behaviours of the polymeric network in water before and after sulfonation (**B**).

In this article, modification of a homogeneous sulfonation method[16,33] to heterogeneous media was described. The previously published technique for sulfonation of 9,10-diphenylanthracene (DPA)[16,33] was transposed to its macromolecular porous analogue (DPA-PAF) successfully. Since the reaction the reaction is performed in acetic acid/water mixture, it is more environmentally friendly and economical when compared to the common pathway of heterogeneous post-sulfonation of porous organic polymers through chlorosulfonic acid in chlorinated solvents. Aside from the macroscopic observations such as excellent water dispersibility after the modification, success of the method was proven by using essential characterization techniques for porous materials such as infra-red spectroscopy, gas sorption (surface area) measurements, and elemental analysis.

2. Experimental

2.1. Chemical Materials and Apparatus

All chemicals are used as received without further purification. Fuming sulfuric acid (Oleum, 30% free SO_3), iodobenzene (98%), tetrahydrofuran (THF, anhydrous, Sure/Seal™, ≥99.9% for the Suzuki-Miyaura reaction), THF (ACS reagent, ≥99.0%, for common use), potassium carbonate ((K_2CO_3), ACS reagent, ≥99.0%), glacial acetic acid (ACS reagent, ≥99.7%), acetic anhydride (ACS reagent ≥98.0%), palladium-tetrakis(triphenylphosphine) (($Pd(PPh_3)_4$), 99%) were bought from Sigma-Aldrich. Tetrakis(4-bromophenyl)methane (>95) and 9,10-Bis(4,4,5,5-tetramethyl-1,3,2-dioxaborolan-2-yl)anthracene (>98%) purchased from TCI Chemicals. 10-Phenylanthracene-9-boronic acid (98%) was received from Alfa Aesar. Water was purified through Mili-Q filter. Gas sorption measurements were employed by using Micromeritics TriStar 3000. Infra-red measurements were conducted via PerkinElmer FTIR spectrophotometer. ThermoScientific Flash 2000 was used for elemental analyses. Bruker 400 MHz DNP nuclear magnetic resonance (NMR) instrument was used to record solid-state cross-polarization magic angle spinning (CP-MAS) 13C spectrum. JEOL JSM-7900F equipped with ULTIM Max 170 from Oxford Instruments was used for scanning electron microscopy (SEM) and energy dispersive X-ray spectroscopy (EDX) analysis.

2.2. Chemistry

2.2.1. Synthesis of DPA-PAF

0.15 g (0.23 mmol) Tetrakis(4-bromophenyl)methane, 0.20 g (0.46 mmol) 9,10-Bis(4,4,5,5-tetramethyl-1,3,2-dioxaborolan-2-yl)anthracene, 36 mg (0.03 mmol) $Pd(PPh_3)_4$ were put in a 100 mL 3 neck round bottom flask in glovebox. The sealed flask was then removed from the glovebox, to which a reflux condenser was attached under N_2 flow. After addition of 15 mL anhydrous THF as solvent, introduction of previously degassed (30 mins N_2 bubbling) 2.32 mL 2 M $K_2CO_{3\,(aq)}$ was employed. The sealed flask was refluxed for 3 days, and cooled down to room temperature to introduce the first endcapper, 0.28 g (0.92 mmol) 10-Phenylanthracene-9-boronic acid (98%) as its dispersion in 5 mL anhydrous THF under inert atmosphere. The mixture was then heated to 85ºC for 2 hours, and cooled down to add second endcapper, 0.57 g (0.31 mL, 2.8 mmol) iodobenzene, and the mixture was refluxed again for 2 hours. After cooling down to room temperature, the precipitate was collected via filtration, and the solid was washed with MeOH, water, THF, $CHCl_3$, and finally again MeOH 50 mL for each. Then, the solid was put in Soxhlet extraction apparatus to be extensively purified by using MeOH overnight. The final greenish-pale yellow powder yielded 0.15 g in 97%.

2.3.2. Synthesis of DPA-PAF-SO_3Na

90 mg DPA-PAF was put in a 25 mL round bottom flask, and dispersed in 2.7 mL CH_3COOH and 0.3 mL $(CH_3CO)_2O$ mixture. The dispersion put in ice bath to cool down prior to adding 0.15 mL oleum slowly. The mixture was then removed from the ice bath, and refluxed at 130°C for an hour. In following, the flask cooled down to room temperature to introduce 3 mL deionized water and 0.27 g NaCl. The mixture was refluxed at 130°C for an hour again, cooled down, neutralized by using 1 M $NaOH_{(aq)}$. The neutralized heterogeneous mixture was filtered, and the precipitate was washed with

deionized water. Washing the powder was continued in a centrifuge tube 3 times with 10 mL water. The remaining precipitate was 62 mg.

3. Results and Discussion

Even though *PAF-style* networks of DPA were presented previously, those porous materials were produced by using random co-polymerization through Yamamoto coupling, therefore, the repeating co-monomers are randomly placed.[34,35] Here, the phenyls of tetraphenyl methane provide the functionalization of anthracene on 9,10 positions, therefore, final compound can be identified as the porous polymer of DPA connected by only one carbon. The synthesis of parent network, DPA-PAF, was conducted by using Suzuki-Miyaura polymerization technique between a di-boronic acid ester derivative of anthracene (9,10-Bis(4,4,5,5-tetramethyl-1,3,2-dioxaborolan-2-yl)anthracene) and a tetra-halo derivative of tetraphenyl methane (Tetrakis(4-bromophenyl)methane) by modifying a previously published technique[36] for the CMP of DPA (see Figure 1A for the reaction scheme, and experimental part for details). ^{13}C CP-MAS NMR of the final compound indicated the quaternary peak of tetraphenyl methane (TPM) at 64 ppm with another characteristic peak at 145 ppm, and additional lower intensity aromatic C-C connection peak between anthracene and benzene of TPM at 136 ppm (Figure S1). Other high intensity two high intensity peaks at 129 ppm and 125 ppm should be coming from the hydrogen attached carbons of anthracene and TPM units, which is in agreement with the literature.[34,35] Sulfonation of DPA-PAF via oleum in aqueous media was then employed to reach the final compound, DPA-PAF-SO_3Na, which shows extremely good hydrophilicity when compared to the fully hydrophobic DPA-PAF (see Figure 1B, and also the video uploaded as supporting information).

Aside from visual observations, successful introduction of sulfonate groups was proven by using several analytic methods. The thermal elemental analysis (EA, only can detect CHNS) indicated presence of sulfur after sulfonation, which is a solid proof of the functionalization (Table 1). The EA for the pristine DPA-PAF gave a value **C** 88.3%; **H** 4.8% (theoretical value for DPA monomer is **C** 94.5% **H** 5.5%) whereas the result for DPA-PAF-SO_3Na was **C** 59.0%; **H** 3.7%; **S** 5.4% (theoretical value for monomeric monosulfonated DPA-SO_3Na[16,33]: **C** 72.2%; **H** 4.0%; **S** 7.4%; **O** 11.1%; **Na** 5.3%). Even though determination of the exact elemental composition of such polymeric networks is not entirely possible,[37] the results obtained from the EA measurement indicated at least 73% ((5.4/7.4)×100 ≅ 73%) of functionalization if monosulfonation of DPA[16,33] is considered as reference.

Table 1. EA analysis results of DPA-PAF and DPA-PAF-SO_3Na

	C%	**H%**	**S%**	**Na%**	**O%**
Theoretical[a] DPA	94.5	5.5	-	-	-
EA DPA-PAF	88.3	4.8	-	-	-
SEM-EDX DPA-PAF	95.1	-	0.1[b]	0.6[b]	2.2[b]
Theoretical[a] DPA-SO_3Na	72.2	4.0	7.4	5.3	11.1
EA DPA-PAF-SO_3Na	59.0	3.7	5.4	-	-
SEM-EDX DPA-PAF-SO_3Na	74.2	-	5.9	4.5	13.0

[a]The values calculated from the corresponding monomers by using ChemSketch software. [b]The presence of the addressed elements can be to be due to the contamination from ethanol, which was used during sample preparation (the samples were prepared by drop casting from their ethanol dispersions.

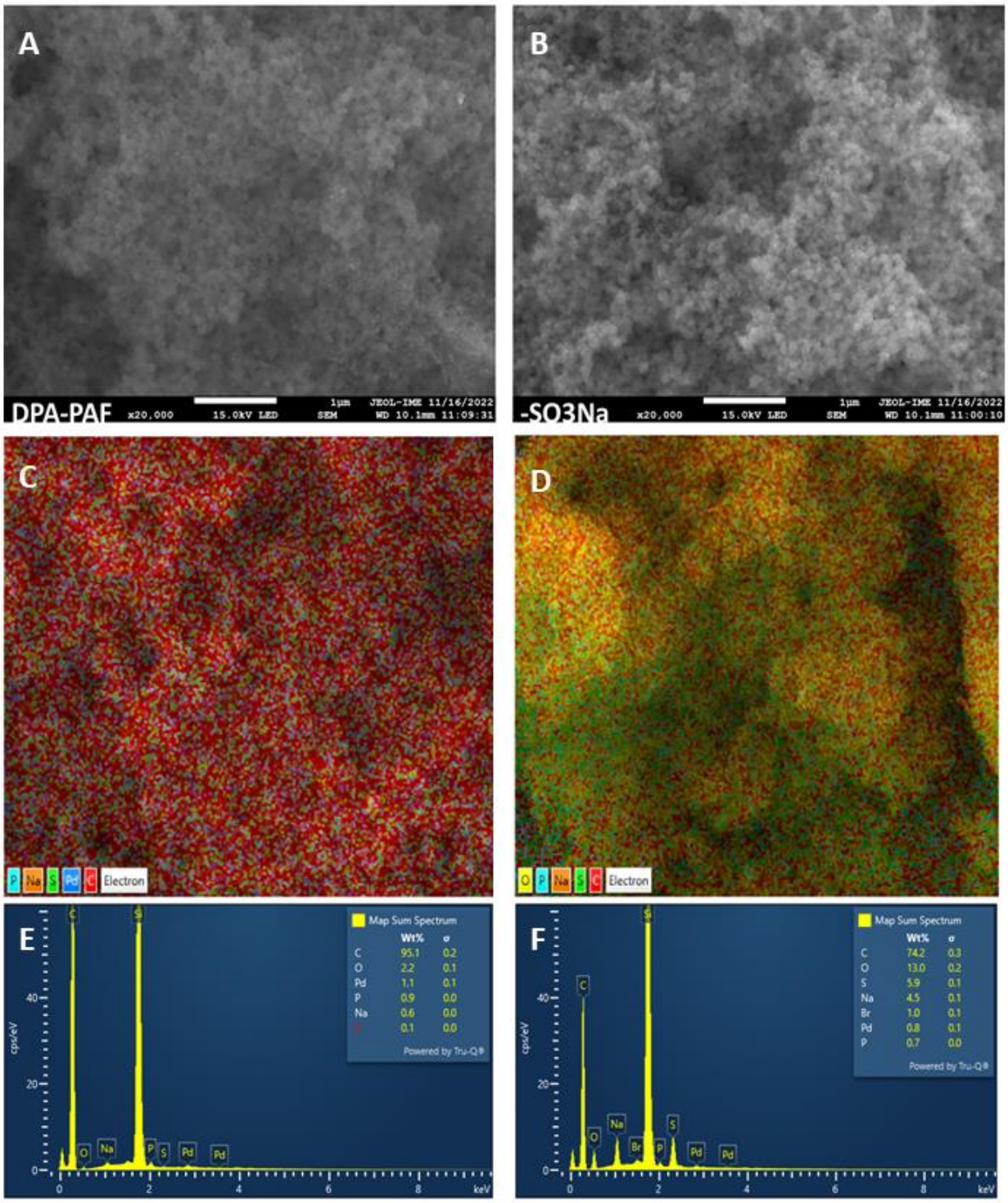

Figure 2. SEM-EDX details for the pristine and modified polymers: SEM images (scales 1 µm) of DPA-PAF (**A**) and DPA-PAF-SO_3Na (**B**), EDX mapping images (color code order of the elements listed left bottom P, Na, S, Pd, C) of DPA-PAF (**C**) and DPA-PAF-SO_3Na (color code order of the elements listed left bottom O, P, Na, S, C) (**D**), EDX spectra of DPA-PAF (E) and DPA-PAF-SO_3Na (F). More detailed images can be seen from the SI (Figure S2-S4).

Another elemental analysis technique, energy dispersive X-ray spectroscopy (EDX), was performed to detect elemental composition through scanning electron microscopy (SEM). The results obtained by this technique was closer to the theoretical values, and also helped to determine the amounts

of Na and O. EDX of DPA-PAF gave a nearly full carbon content at 95.1% (the S, Na, O impurities probably occurred during sample preparation for EDX measurements). After sulfonation, the carbon content dropped to 74.2% while S, Na, O percentages raised to 5.9, 4.5, and 13.0, respectively. Depending on these values, success of sulfonation can be calculated as %80 ((5.9/7.4)×100 ≅ 80%). Moreover, EDX mapping images in Figure 2 illustrated the high amount of functionalization via reduction of red segments (color code for C) and increase of green places (color code for S) on the surface. Additionally, detection of some amounts of Br endgroups despite the endcaping, and also presence of Pd impurities despite extensive Soxhlet extraction, even after oleum treatment for sulfonation in case of DPA-PAF-SO_3Na, can be interesting for further studies (e.g. photocatalytic water splitting[38–40]) in the field.

Since infra-red (IR) spectroscopy is one the most essential techniques in organic chemistry to characterize functional groups, IR spectra of DPA-PAF and DPA-PAF-SO_3Na were compared (Figure 3). Indeed, significant changes were detected after sulfonation of the parent compound. The characteristic peaks of sulfonate groups at 1093 cm^{-1} due to S−O, and the doublet at 1218 cm^{-1} and 1178 cm^{-1} due to S=O strechings clearly demonstrated the presence of sulfonate groups.[41] The shift of the peak from 1020 to 1041 cm^{-1}, probably occurring from the electronic effect of sulfonate groups on the *in-plane bending* vibrations of neighboring aromatic C-H,[42] was similar to the observations in the literature.[30] The altered intensity pattern of C=C−C aromatic ring vibrations at 1507 cm^{-1}, 1438 cm^{-1}, and 1390 cm^{-1} should be due to the appeared structural asymmetry after sulfonation.[42,43] The intense peaks at 3430 cm^{-1} and 1630 cm^{-1} should be coming from stretching and bending vibrations of the ambient water trapped in the polymeric network as a result of increased hydrophilicity.[31,44]

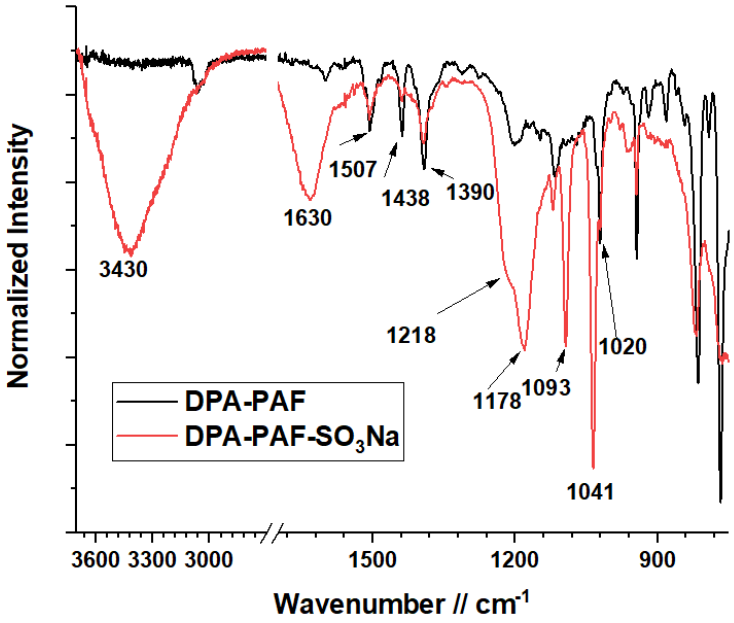

Figure 3. IR Spectra of DPA-PAF and DPA-PAF-SO_3Na

N_2 gas sorption measurements were employed to detect the specific surface area of the polymeric networks DPA-PAF and DPA-PAF-SO_3Na, which also confirmed the formation of sulfonate groups. The less gas uptake in the low relative pressures (P/P_0) on the isotherm of DPA-PAF-SO_3Na when compared to the parent DPA-PAF clearly indicates the formation of sulfonate groups along the skeleton (Figure 4A). Indeed, the drop of the calculated Brunauer–Emmett–Teller (BET) surface area from 707 m^2g^{-1} to 356 m^2g^{-1} was not surprising since the formed sulfonate groups reduce the pore accessibility. The NL-DFT pore-size distribution also demonstrated the lack of accessibility of micropores via the reduced intensity of the contribution around 1.1 nm (Figure 4B).

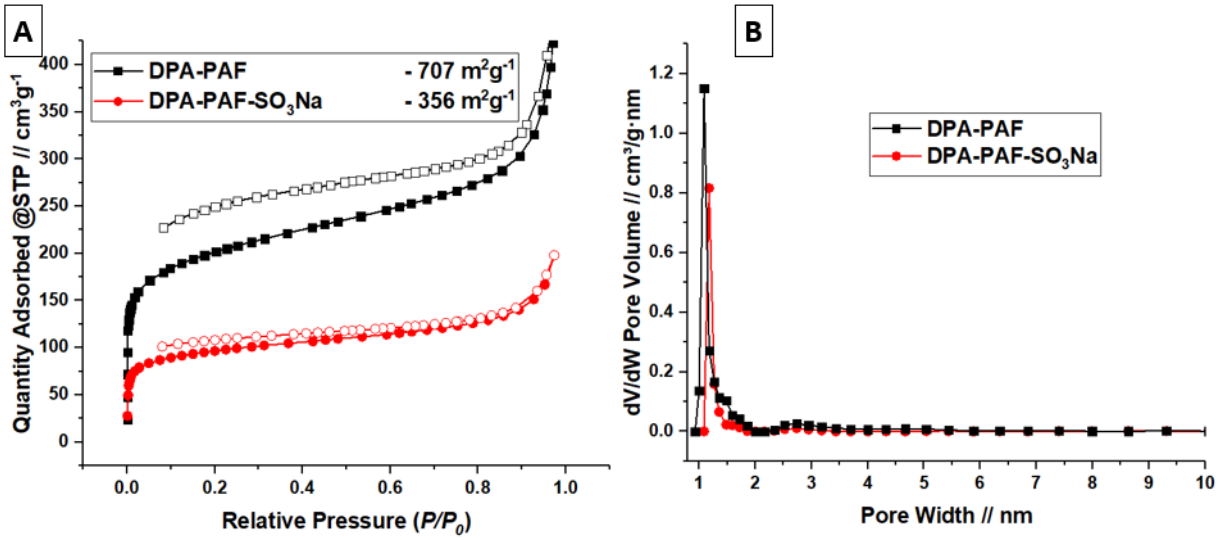

Figure 4. N_2 gas sorption isotherms (**A**) and NL-DFT pore-size distributions (**B**) of DPA-PAF and DPA-PAF-SO_3Na

4. Conclusion

Successful post-synthetic sulfonation of a high surface area porous polymeric network named DPA-PAF was described in this article. The post-synthesis was carried out by using fuming sulfuric acid (oleum) in aqueous media to form DPA-PAF-SO_3Na. Drastically improved hydrophilicity after the reaction indicated the formation of sulfonate groups along the structure. At least 73% functionalization was calculated by the EA, and 80% by the EDX measurements. Comparison of the IR spectra of DPA-PAF and DPA-PAF-SO_3Na clearly demonstrated presence of sulfonate groups. Additionally, the altered IR vibrations coming from the neighboring moieties clearly indicated electronical changes and enhanced asymmetry along the backbone. Drop of the measured BET surface area from area from 707 m^2g^{-1} to 356 m^2g^{-1} after sulfonation was detected due to the pore blockage of formed sulfonate groups, which was also confirmed by NL-DFT pore size distribution. The presented post-synthetic sulfonation method is an environmentally friendly and efficient alternative pathway to the conventionally used chlorosulfonic acid in chlorinated solvents. The functionalization made the hydrophobic porous organic polymer more hydrophilic, therefore, more promising for the applications in aqueous media such as photocatalytic water splitting.

Acknowledgements

Author would like to thank Prof. Kasper Moth-Poulsen from Chalmers University of Technology and Institut de Ciència de Materials de Barcelona (ICMAB-CSIC) for his support, and Swedish research council for sustainable development (FORMAS) for the funding. Additionally, author thanks to Dr. Marta Liras and Fernando Pico from IMDEA Energy for the SEM-EDX measurements.

Supporting Information

Supporting information accompanies this paper on http://www.acgpubs.org/journal/organic-communications

ORCID
Hakan Bildirir: 0000-0001-9909-4585

References

[1] Slater, A. G.; Cooper, A. I. Function-Led Design of New Porous Materials. *Science (80-.).* **2015**, *348* (6238), aaa8075. doi:10.1126/science.aaa8075.

[2] Silaghi, M. C.; Chizallet, C.; Raybaud, P. Challenges on molecular aspects of dealumination and desilication of zeolites. *Micropor. Mesopor. Mater.* **2014**, *191*, 82–96.

[3] Hendon, C. H.; Rieth, A. J.; Korzyński, M. D.; Dincă, M. Grand challenges and future opportunities for metal-organic frameworks. *ACS Cent. Sci.* **2017**, *3*, 554–563.

[4] Farha, O. K.; Eryazici, I.; Jeong, N. C.; Hauser, B. G.; Wilmer, C. E.; Sarjeant, A. A.; Snurr, R. Q.; Nguyen, S. T.; Yazaydin, A. Ö.; Hupp, J. T. Metal-organic framework materials with ultrahigh surface areas: is the sky the limit? *J. Am. Chem. Soc.* **2012**, *134*, 15016–15021.

[5] Thomas, A. Much Ado about nothing – a decade of porous materials research. *Nat. Commun.* **2020**, *11* (*1*), 4985. doi:10.1038/s41467-020-18746-5.

[6] Xiao, J.; Liu, X.; Pan, L.; Shi, C.; Zhang, X.; Zou, J. J. Heterogeneous photocatalytic organic transformation reactions using conjugated polymers-based materials. *ACS Catal.* **2020**, *10* (*20*), 12256–12283.

[7] Bildirir, H.; Gregoriou, V. G.; Avgeropoulos, A.; Scherf, U.; Chochos, C. L. Porous organic polymers as emerging new materials for organic photovoltaic applications: current status and future challenges. *Mater. Horizons* **2017**, *4* (*4*), 546–556.

[8] Bildirir, H. Have Covalent organic framework films revealed their full potential? *Crystals* **2021**, *11* (*7*), 762. doi:10.3390/cryst11070762.

[9] Chaoui, N.; Trunk, M.; Dawson, R.; Schmidt, J.; Thomas, A. Trends and challenges for microporous polymers. *Chem. Soc. Rev.* **2017**, *46* (*11*), 3302–3321.

[10] Zhou, Y. B.; Zhan, Z. P. Conjugated microporous polymers for heterogeneous catalysis. *Chem. An Asian J.* **2018**, *13* (*1*), 9–19.

[11] Dadashi-Silab, S.; Bildirir, H.; Dawson, R.; Thomas, A.; Yagci, Y. Microporous thioxanthone polymers as heterogeneous photoinitiators for visible light induced free radical and cationic polymerizations. *Macromolecules* **2014**, *47* (*14*), 4607–4614.

[12] Rose, M. Nanoporous polymers: bridging the gap between molecular and solid catalysts? *ChemCatChem* **2014**, *6* (*5*), 1166–1182.

[13] Cheng, J.-Z.; Tan, Z.-R.; Xing, Y.-Q.; Shen, Z.-Q.; Zhang, Y.-J.; Liu, L.-L.; Yang, K.; Chen, L.; Liu, S.-Y. Exfoliated conjugated porous polymer nanosheets for highly efficient photocatalytic hydrogen evolution. *J. Mater. Chem. A* **2021**, *9* (*9*), 5787–5795.

[14] Molina, A.; Patil, N.; Ventosa, E.; Liras, M.; Palma, J.; Marcilla, R. New anthraquinone-based conjugated microporous polymer cathode with ultrahigh specific surface area for high-performance lithium-ion batteries. *Adv. Funct. Mater.* **2020**, *30*, 1908074. doi:10.1002/adfm.201908074.

[15] Banerjee, T.; Lotsch, B. V. The wetter the better. *Nat. Chem.* **2018**, *10* (*12*), 1175–1177.

[16] Bharmoria, P.; Hisamitsu, S.; Sasaki, Y.; Kang, T. S.; Morikawa, M. A.; Joarder, B.; Moth-Poulsen, K.; Bildirir, H.; Mårtensson, A.; Yanai, N.; Kimizuka, N. Photon upconverting bioplastics with high efficiency and in-air durability. *J. Mater. Chem. C* **2021**, *9*, 11655–11661.

[17] Lin, K.; Wang, Z.; Hu, Z.; Luo, P.; Yang, X.; Zhang, X.; Rafiq, M.; Huang, F.; Cao, Y. Amino-functionalised conjugated porous polymers for improved photocatalytic hydrogen evolution. *J. Mater. Chem. A* **2019**, *7*, 19087–19093.

[18] Segura, J. L.; Royuela, S.; Mar Ramos, M. Post-synthetic modification of covalent organic frameworks. *Chem. Soc. Rev.* **2019**, *48* (*14*), 3903–3945.

[19] Lu, W.; Yuan, D.; Sculley, J.; Zhao, D.; Krishna, R.; Zhou, H. C. Sulfonate-Grafted porous polymer networks for preferential Co 2 adsorption at low pressure. *J. Am. Chem. Soc.* **2011**, *133* (*45*), 18126–18129.

[20] James, A. M.; Harding, S.; Robshaw, T.; Bramall, N.; Ogden, M. D.; Dawson, R. Selective Environmental remediation of strontium and cesium using sulfonated hyper-cross-linked polymers (SHCPs). *ACS Appl. Mater. Interface.* **2019**, *11* (*25*), 22464–22473.

[21] Bhanja, P.; Palui, A.; Chatterjee, S.; Kaneti, Y. V.; Na, J.; Sugahara, Y.; Bhaumik, A.; Yamauchi, Y. Crystalline porous organic polymer bearing $-SO_3H$ functionality for high proton conductivity. *ACS Sustain. Chem. Eng.* **2020**, *8* (*6*), 2423–2432.

[22] Kang, D. W.; Kang, M.; Moon, M.; Kim, H.; Eom, S.; Choe, J. H.; Lee, W. R.; Hong, C. S. PDMS-coated hypercrosslinked porous organic polymers modified via double postsynthetic acidifications for ammonia capture. *Chem. Sci.* **2018**, *9* (*33*), 6871–6877.

[23] Kang, D. W.; Lim, K. S.; Lee, K. J.; Lee, J. H.; Lee, W. R.; Song, J. H.; Yeom, K. H.; Kim, J. Y.; Hong, C. S. Cost-effective, high-performance porous-organic-polymer conductors functionalized with sulfonic acid groups by direct postsynthetic substitution. *Angew. Chemie Int. Ed.* **2016**, *55* (*52*), 16123–16126.

[24] Kang, S. Y.; Lim, Y. N.; Cheong, Y.-J.; Lee, S. M.; Kim, H. J.; Ko, Y.-J.; Lee, B. Y.; Jang, H.-Y.; Son, S. U. nanoseeded catalytic terpolymerization of co, ethylene, and propylene by size-controlled SiO_2@sulfonated microporous organic polymer. *Ind. Eng. Chem. Res.* **2017**, *56* (*37*), 10235–10241.

[25] Kalla, R. M. N.; Kim, M.-R.; Kim, I. Sulfonic acid-functionalized, hyper-cross-linked porous polyphenols as recyclable solid acid catalysts for esterification and transesterification reactions. *Ind. Eng. Chem. Res.* **2018**, *57* (*34*), 11583–11591.

[26] Park, N.; Lim, Y. N.; Kang, S. Y.; Lee, S. M.; Kim, H. J.; Ko, Y.-J.; Lee, B. Y.; Jang, H.-Y.; Son, S. U. Hollow and microporous organic polymers bearing sulfonic acids: antifouling seed materials for polyketone synthesis. *ACS Macro Lett.* **2016**, *5* (*12*), 1322–1326.

[27] Du, M.; Agrawal, A. M.; Chakraborty, S.; Garibay, S. J.; Limvorapitux, R.; Choi, B.; Madrahimov, S. T.; Nguyen, S. T. Matching the activity of homogeneous sulfonic acids: the fructose-to-hmf conversion catalyzed by hierarchically porous sulfonic-acid-functionalized porous organic polymer (pop) catalysts. *ACS Sustain. Chem. Eng.* **2019**, *7* (*9*), 8126–8135.

[28] Li, Z.; Yao, Y.; Wang, D.; Hasan, M. M.; Suwansoontorn, A.; Li, H.; Du, G.; Liu, Z.; Nagao, Y. Simple and universal synthesis of sulfonated porous organic polymers with high proton conductivity. *Mater. Chem. Front.* **2020**, *4* (*8*), 2339–2345.

[29] Welton, T. Solvents and sustainable chemistry. *Proc. R. Soc. A Math. Phys. Eng. Sci.* **2015**, *471* (*2183*), 20150502. doi:10.1098/rspa.2015.0502.

[30] Goesten, M. G.; Szécsényi, À.; de Lange, M. F.; Bavykina, A. V; Gupta, K. B. S. S.; Kapteijn, F.; Gascon, J. Sulfonated porous aromatic frameworks as solid acid catalysts. *ChemCatChem* **2016**, *8* (*5*), 961–967.

[31] Klumpen, C.; Gödrich, S.; Papastavrou, G.; Senker, J. Water mediated proton conduction in a sulfonated microporous organic polymer. *Chem. Commun.* **2017**, *53* (*54*), 7592–7595.

[32] Zhao, W.; Jiao, Y.; Gao, R.; Wu, L.; Cheng, S.; Zhuang, Q.; Xie, A.; Dong, W. Sulfonate-grafted conjugated microporous polymers for fast removal of cationic dyes from water. *Chem. Eng. J.* **2020**, *391*, 123591. doi:10.1016/j.cej.2019.123591.

[33] Hisamitsu, S.; Yanai, N.; Kimizuka, N. Photon-Upconverting ionic liquids: effective triplet energy migration in contiguous ionic chromophore arrays. *Angew. Chemie Int. Ed.* **2015**, *54* (*39*), 11550–11554.

[34] Xiang, Z.; Mercado, R.; Huck, J. M.; Wang, H.; Guo, Z.; Wang, W.; Cao, D.; Haranczyk, M.; Smit, B. Systematic Tuning and multifunctionalization of covalent organic polymers for enhanced carbon capture. *J. Am. Chem. Soc.* **2015**, *137* (*41*), 13301–13307.

[35] Perego, J.; Pedrini, J.; Bezuidenhout, C. X.; Sozzani, P. E.; Meinardi, F.; Bracco, S.; Comotti, A.; Monguzzi, A. Engineering Porous emitting framework nanoparticles with integrated sensitizers for low-power photon upconversion by triplet fusion. *Adv. Mater.* **2019**, *31*(*40*), 1903309. doi:10.1002/adma.201903309.

[36] Edhborg, F.; Bildirir, H.; Bharmoria, P.; Moth-Poulsen, K.; Albinsson, B. Intramolecular triplet-triplet annihilation photon upconversion in diffusionally restricted anthracene polymer. *J. Phys. Chem. B* **2021**, *125* (*23*), 6255–6263.

[37] Zhang, Q.; Yang, Y.; Zhang, S. Novel functionalized microporous organic networks based on triphenylphosphine. *Chem. A. Eur. J.* **2013**, *19* (*30*), 10024–10029.

[38] Kosco, J.; Sachs, M.; Godin, R.; Kirkus, M.; Francas, L.; Bidwell, M.; Qureshi, M.; Anjum, D.; Durrant, J. R.; McCulloch, I. The Effect of residual palladium catalyst contamination on the photocatalytic hydrogen evolution activity of conjugated polymers. *Adv. Energy Mater.* **2018**, *8* (*34*), 1802181. doi:10.1002/aenm.201802181.

[39] Chang, C.-L.; Elewa, A. M.; Wang, J. H.; Chou, H.-H.; EL-Mahdy, A. F. M. Donor–acceptor conjugated microporous polymers based on thiazolo[5,4-d]thiazole building block for high-performance visible-light-induced H_2 production. *Micropor. Mesopor. Mater.* **2022**, *345*, 112258. doi:10.1016/j.micromeso.2022.112258.

[40] Wang, Y.; Vogel, A.; Sachs, M.; Sprick, R. S.; Wilbraham, L.; Moniz, S. J. A.; Godin, R.; Zwijnenburg, M. A.; Durrant, J. R.; Cooper, A. I.; Tang, J. Current understanding and challenges of solar-driven hydrogen generation using polymeric photocatalysts. *Nat. Energy* **2019**, *4* (*9*), 746–760.

[41] Fujimori, K. The Infrared spectra of alkane-1-sulfonates. *Bull. Chem. Soc. Jpn.* **1959**, *32* (*8*), 850–852.

[42] Coates, J. Interpretation of Infrared Spectra, A Practical Approach. In *Encyclopedia of Analytical Chemistry*; 2006. doi:10.1002/9780470027318.a5606.

[43] Bildirir, H. Effect of Crosslinking patterns on the properties of conjugated microporouspolymers. *Turk. J. Chem.* **2019**, *43* (*2*), 730–739.
[44] Seki, T.; Chiang, K.-Y.; Yu, C.-C.; Yu, X.; Okuno, M.; Hunger, J.; Nagata, Y.; Bonn, M. The bending mode of water: a powerful probe for hydrogen bond structure of aqueous systems. *J. Phys. Chem. Lett.* **2020**, *11* (*19*), 8459–8469.